



# The Changing-look Quasar Mrk 590 Is Awakening

S. Mathur<sup>1,2</sup> , K. D. Denney<sup>3</sup>, A. Gupta<sup>1,4</sup>, M. Vestergaard<sup>5,6</sup>, G. De Rosa<sup>7</sup>, Yair Krongold<sup>8</sup>, F. Nicastro<sup>9</sup> , J. Collinson<sup>10</sup>,  
M. Goad<sup>11</sup>, K. Korista<sup>12</sup>, R. W. Pogge<sup>1,2</sup> , and B. M. Peterson<sup>1,2,7</sup> 

<sup>1</sup> Department of Astronomy, The Ohio State University, 140 West 18th Avenue, Columbus, OH 43210, USA

<sup>2</sup> Center for Cosmology and AstroParticle Physics, The Ohio State University, 191 West Woodruff Avenue, Columbus, OH 43210, USA

<sup>3</sup> Illumination Works, Columbus, OH, USA; [denney@astronomy.ohio-state.edu](mailto:denney@astronomy.ohio-state.edu)

<sup>4</sup> Department of Biological and Physical Sciences, Columbus State Community College, Columbus, OH 43215, USA

<sup>5</sup> Dark Cosmology Centre, Niels Bohr Institute, University of Copenhagen, Juliane Maries Vej 30, DK-2100 Copenhagen Ø, Denmark

<sup>6</sup> Steward Observatory, 933 N. Cherry Avenue, Tucson, AZ 85721, USA

<sup>7</sup> Space Telescope Science Institute, Baltimore, MD 21218, USA

<sup>8</sup> Instituto de Astronomía, Universidad Nacional Autónoma de México, Ciudad de México, Mexico

<sup>9</sup> Istituto Nazionale di Astrofisica (INAF) Osservatorio Astronomico di Roma, via Frascati, Monte Porzio Catone I-00078, RM, Italy

<sup>10</sup> Centre for Extragalactic Astronomy, Department of Physics, Durham University, South Road, Durham DH1 3LE, UK

<sup>11</sup> Department of Physics and Astronomy, University of Leicester, University Road, Leicester LE1 7RH, UK

<sup>12</sup> Department of Physics, Western Michigan University, Kalamazoo, MI 49008, USA

Received 2018 May 21; revised 2018 August 20; accepted 2018 August 27; published 2018 October 19

## Abstract

Mrk 590 was originally classified as a Seyfert 1 galaxy, but then it underwent dramatic changes: the nuclear luminosity dropped by over two orders of magnitude and the broad emission lines all but disappeared from the optical spectrum. Here we present follow-up observations to the original discovery and characterization of this “changing-look” active galactic nucleus (AGN). The new *Chandra* and *Hubble Space Telescope* observations from 2014 show that Mrk 590 is awakening, changing its appearance again. While the source continues to be in a low state, its soft excess has re-emerged, though not to the previous level. The UV continuum is brighter by more than a factor of two and the broad Mg II emission line is present, indicating that the ionizing continuum is also brightening. These observations suggest that the soft excess is not due to reprocessed hard X-ray emission. Instead, it is connected to the UV continuum through warm Comptonization. Variability of the Fe K $\alpha$  emission lines suggests that the reprocessing region is within  $\sim 10$  lt-yr or 3 pc of the central source. The change in AGN type is neither due to obscuration nor due to one-way evolution from Type 1 to Type 2, as suggested in the literature, but may be related to episodic accretion events.

**Key words:** galaxies: active – galaxies: nuclei – quasars: emission lines – quasars: individual (Mrk 590) – ultraviolet: galaxies – X-rays: galaxies

## 1. Introduction

Active galactic nuclei (AGNs) are characterized by continuum emission across the electromagnetic spectrum and strong emission lines in the UV, optical, and near-IR. AGNs with both broad and narrow emission lines are classified as “Type 1” and those with only narrow emission lines as “Type 2,” and this difference is usually attributed to our viewing angle relative to an obscuring midplane. AGNs are also known to be variable sources, showing variability in the continuum as well as in emission lines. The continuum variability is observed on both short and long timescales, but the variability amplitude is usually small, of the order of  $\sim 20\%$  over a year for low-luminosity AGNs (i.e., with Seyfert-like luminosity of about  $10^{41}$ – $10^{44}$  erg s $^{-1}$ ). The emission-line variations usually track the continuum variations, but see Goad et al. (2016).

A special class of AGN that has recently been gaining recognition has been termed “changing-look quasars.”<sup>13</sup> Their broad emission lines are observed to appear or disappear together with large changes in continuum luminosity. The changes in the emission-line spectra are such that they change type, e.g., from “Type 1” to “Type 2,” and this is clearly an

*intrinsic* change, implying that “type” is not always associated with viewing angle. This phenomenon has become of recent interest due to a combination of several serendipitous discoveries of changing-look AGNs (e.g., Shappee et al. 2014; Denney et al. 2014; LaMassa et al. 2015) and the growing availability of large spectroscopic quasar databases with long time-baselines of multi-epoch photometry and spectroscopy. These rare occurrences have the potential to contribute to our limited understanding of the central engines of active galaxies. Systematic searches of databases such as the SDSS/BOSS/TDSS have begun to uncover more changing-look quasars at larger redshifts and have led to predictions of the possible occurrence rates for quasars to change type (MacLeod et al. 2016; Runnoe et al. 2016).

Changing-look quasars are of particular interest for their potential to shed light on the physical origin of quasar variability and the details of accretion, since they have undergone such an extreme apparent change. Additionally, what is the role these objects play in the accretion history of the black hole (BH)—are we observing the beginning/end of a quasar phase? What role do these objects play in the larger context of galaxy and BH coevolution? Recent investigations of changing-look quasars have tried to use the observations before and after the change and any additional data available on the few known sources to test whether or not the changes are due to changes in accretion rate or obscuration, and to determine whether the quasar is turning on for the first time,

<sup>13</sup> We make no distinction among the terms quasar, AGN, and Seyfert galaxy—all are objects that contain a central black hole that is actively accreting sufficient matter to shine as a point source and that, to first order, produce the same emission characteristics.

reviving after a period of quiescence, or something else. In all cases so far, obscuration has not been identified as the major cause of changing look. Instead, a significant increase (decrease) in the mass accretion rate is the most favored explanation for the appearance (disappearance) of the broad emission lines.

The nearby, low-luminosity AGN Markarian 590 (Mrk 590 hereafter) remains an interesting case of a changing-look quasar in the local universe. Denney et al. (2014; D14 hereafter) have described the initial set of observations that catalog this object’s observed history and “change,” where it went from being a strong broad-line emitter three decades ago, allowing a reverberation mapping-based direct BH mass measurement to be made ( $(4.75 \pm 0.74) \times 10^7 M_{\odot}$ , Peterson et al. 2004), to being broad-line weak—the optical broad lines all but disappeared—in the past decade. Mrk 590 also shows the presence of ultrafast outflows in the X-ray band (Gupta et al. 2015). We have obtained additional UV and X-ray spectra since those presented by D14 that we describe in Sections 2 and 3. Implications of our results are discussed in Section 4 and we show that the “soft X-ray excess,” observed in a large fraction of AGNs, is not due to the reprocessing of hard X-ray continuum, but is instead a result of thermal Comptonization of UV photons. We also argue that the changing-look phenomenon is a normal event in the duty cycle of “normal” quasars.

## 2. Chandra Spectroscopy

Mrk 590 was observed by *Chandra* for 68.87 ks on 2014 November 15 (ObsID 16109). This is longer than the 30 ks initial Director’s Discretionary Time (DDT) observation presented by D14, but the observing parameters were otherwise kept the same. We observed with ACIS-S/HETG; the grating was inserted in front of the detector in order to mitigate pile-up, if any. The data were reduced with CIAO following the normal procedure and analyzed using XSPEC. A Galactic column density of  $N_{\text{H}} = 2.7 \times 10^{20} \text{ cm}^{-2}$  was included in all fits and was held fixed. All the quoted errors are for 90% confidence, unless noted otherwise. Figure 1 shows the new, 2014 spectrum, together with the 2013 spectrum presented by D14, and the previous “high state” spectrum observed in 2004. The source continues to be in a low state in 2014, so the quality of the high-resolution grating spectrum is too poor to perform useful science. Hence we present the zeroth-order spectrum here, as was done by D14.

A simple absorbed power-law model did not provide a good fit to the 2014 *Chandra* spectrum. The residuals to this fit are shown in Figure 2, and clearly show a soft excess, so we added a blackbody component to the model. Clear residuals were also observed around 6 keV, so following Longinotti et al. (2007) we added two Gaussian emission lines at rest-frame 6.4 keV and 6.7 keV to represent neutral and ionized Fe K $\alpha$  emission lines, respectively. The resulting fit was good ( $\chi^2_{\nu} = 1.0$  for 104 degrees of freedom); the parameters of the fit are presented in Table 1 and the spectra are shown in Figures 3 and 4. Longinotti et al. (2007) required a third emission line at 7 keV; our data are not good enough in this energy range to require this line. They also detected a line in the soft X-ray band, at 19 Å (0.65 keV), but we see no evidence of that line.

The flux of the source is  $2.2 \times 10^{-12} \text{ erg s}^{-1} \text{ cm}^{-2}$  at 0.3–10 keV ( $1.9 \times 10^{-12} \text{ erg s}^{-1} \text{ cm}^{-2}$  at 0.5–10 keV and  $2.0 \times 10^{-12} \text{ erg s}^{-1} \text{ cm}^{-2}$  at 0.3–8 keV). This is significantly smaller than the 2002 flux ( $8.4 \times 10^{-12} \text{ erg s}^{-1} \text{ cm}^{-2}$ ) reported by Gallo

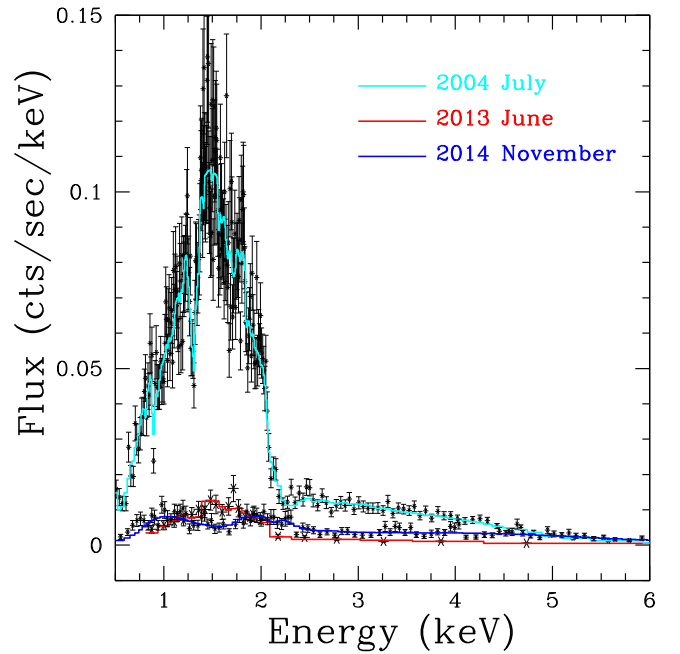


**Figure 1.** *Chandra* spectra of Mrk 590. The high-state spectrum of 2004 and the low-state spectra of 2013 and 2014 are shown. The spectra are fitted with simple power-law continuum models modified by Galactic absorption; these are shown with colored lines to guide the eye. The purpose of this figure is to show that the source continues to remain in the low state in 2014.

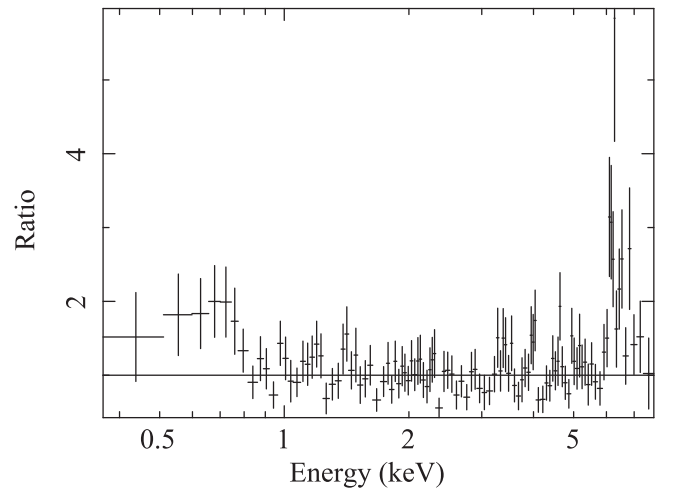


**Figure 2.** Residuals to the 2014 spectrum fitted with an absorbed power-law model. The soft excess is clearly visible below 1 keV. Note also the residuals between 6 and 7 keV, at the locations of Fe lines.

et al. (2006), the 2004 flux ( $11 \times 10^{-12} \text{ erg s}^{-1} \text{ cm}^{-2}$ ) reported by Longinotti et al. (2007), and the *Suzaku* flux of  $6.8 \times 10^{-12} \text{ erg s}^{-1} \text{ cm}^{-2}$  at 2–10 keV reported by Rivers et al. (2012). D14 reported the low state of Mrk 590 with 0.5–10 keV flux of  $1.1 \times 10^{-12} \text{ erg s}^{-1} \text{ cm}^{-2}$ , so compared to our DDT *Chandra* observation in 2013, the source flux appears to have increased slightly, but as shown in Figure 1, the source continues to be in a low state. The flux in the soft excess component is  $3.8 \times 10^{-13} \text{ erg s}^{-1} \text{ cm}^{-2}$  in the 0.3–8 keV band (though it is concentrated below 2 keV), which is 19% of the total. If we restrict to the 0.3–2 keV soft band, then the total flux is  $9.7 \times 10^{-13} \text{ erg s}^{-1} \text{ cm}^{-2}$  while the soft excess flux remains the same as above, making it 39% of the total soft-band flux.

**Table 1**  
*Chandra* Best-fit Spectral Model<sup>a</sup>

Model	Parameter 1	Normalization <sup>b</sup>	Parameter 3
Power law	$\Gamma = 1.6 \pm 0.1$	$(2.4 \pm 0.3) \times 10^{-4}$	
Blackbody	$kT = 0.11^{+0.05}_{-0.02}$ keV	$7^{+7}_{-4} \times 10^{-6}$	
Line 1	$E = 6.4$ keV <sup>c</sup>	$(5 \pm 2) \times 10^{-6}$	EW = $268 \pm 100$ eV
Line 2	$E = 6.7$ keV <sup>c</sup>	$(4 \pm 2) \times 10^{-6}$	EW = $176 \pm 100$ eV

**Notes.**

<sup>a</sup>  $\chi^2_\nu$  for the joint fit is 1.0 for  $\nu = 104$  degrees of freedom.

<sup>b</sup> In units of photons  $\text{s}^{-1} \text{cm}^{-2} \text{keV}^{-1}$ .

<sup>c</sup> Rest frame; parameter frozen.

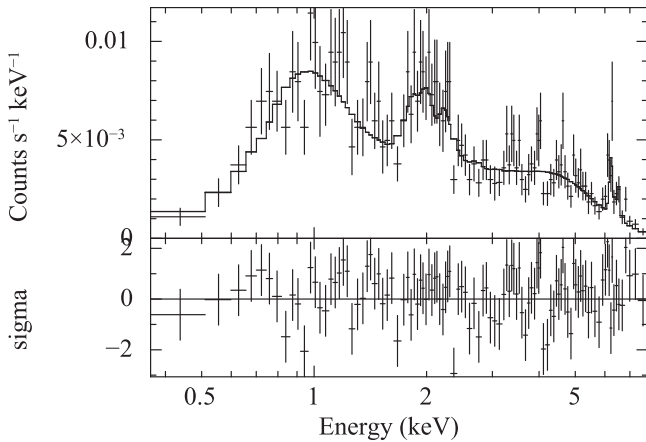


**Figure 3.** The best-fit spectrum and the residuals. The spectrum is fitted with an absorbed power law, a blackbody component to parameterize the soft excess, and two emission lines at 6.4 and 6.7 keV (rest frame).

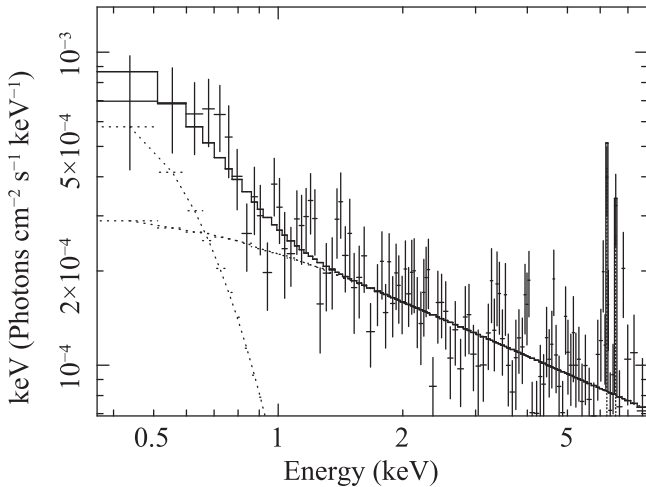


**Figure 4.** The “unfolded” spectrum, i.e., the spectrum without the instrumental response folded in. The model components (power-law continuum, soft excess, and emission lines) are shown as dotted lines.

### 3. *HST*/COS NUV Spectroscopy

We obtained observations with the Cosmic Origins Spectrograph on board the *Hubble Space Telescope* (*HST*) that were coordinated with our approved *Chandra* program. The goal of the COS observations was to observe the portion of the UV spectrum not covered by the initial COS G140L DDT

observations presented by D14. The new observations were obtained on 2014 November 15 with the G230L grating and covered the observed-frame wavelength ranges  $\sim 1670$ – $2175$  Å and  $\sim 2765$ – $3215$  Å. Importantly, this coverage was selected to allow a continuum overlap region with the 2013 G140L spectrum and also to cover the Mg II  $\lambda 2800$  doublet in this object of redshift  $z = 0.026385$ . The G230L spectrum was processed with the standard COS pipelines. Figure 5 shows the G230L COS spectrum, which was modeled with a power-law continuum, a Balmer continuum, and an Fe II template (Vestergaard & Wilkes 2001) as a means to isolate the Mg II emission, with both a narrow-line component and a broad-line component. The width and velocity shift of the narrow-line components of Mg II and N III]  $1750$  Å were tied, allowing only the strength to differ. We also corrected the spectrum for foreground reddening, assuming  $E(B - V) = 0.0367$  mag determined from the dust maps of Schlegel et al. (1998) and the extinction curve of O’Donnell (1994). As can be seen in the figure, the Mg II  $\lambda 2800$  emission line clearly shows a broad component. We measured the FWHM =  $10028 \pm 627$  km  $\text{s}^{-1}$  and the line dispersion  $\sigma = 4000 \pm 790$  km  $\text{s}^{-1}$  for the broad component from the emission-line models.

## 4. Discussion

### 4.1. Soft Excess and the Fe Lines

Over the years, X-ray observations of Mrk 590 have shown that its spectrum is well fit by a power-law continuum, a soft excess, a hard reflection component, and Fe emission lines (Section 1). Rivers et al. (2012), using *Suzaku* data, first noticed that while the hard X-ray continuum of the source remained practically the same as in the historic data, its soft excess had disappeared in 2011. In the 2013 *Chandra* spectrum of D14, there was no evidence of a soft excess either, and the source was in a historically low state. Our new *Chandra* observations show that Mrk 590 continues to be in a low state, but a soft excess has re-emerged. The soft-excess temperature ( $kT = 0.11^{+0.05}_{-0.02}$  keV) is lower than  $kT = 0.18 \pm 0.01$  keV seen in the 2007 *XMM-Newton* spectrum reported by Longinotti et al. (2007) and Rivers et al. (2012). The soft-excess luminosity of  $5 \times 10^{40}$  erg  $\text{s}^{-1} \text{cm}^{-2}$  is also an order of magnitude lower than the 2007 value of  $(8 \pm 1) \times 10^{41}$  erg  $\text{s}^{-1} \text{cm}^{-2}$ , but higher than the upper limit derived from the 2011 *Suzaku* spectra of  $(3 \pm 1) \times 10^{40}$  erg  $\text{s}^{-1} \text{cm}^{-2}$  (Rivers et al. 2012). Thus the soft excess seems to have returned, but not to the “normal” level seen in the historical high state.

In Mathur et al. (2017 and references therein) we discussed various models of the soft excess, which we briefly discuss

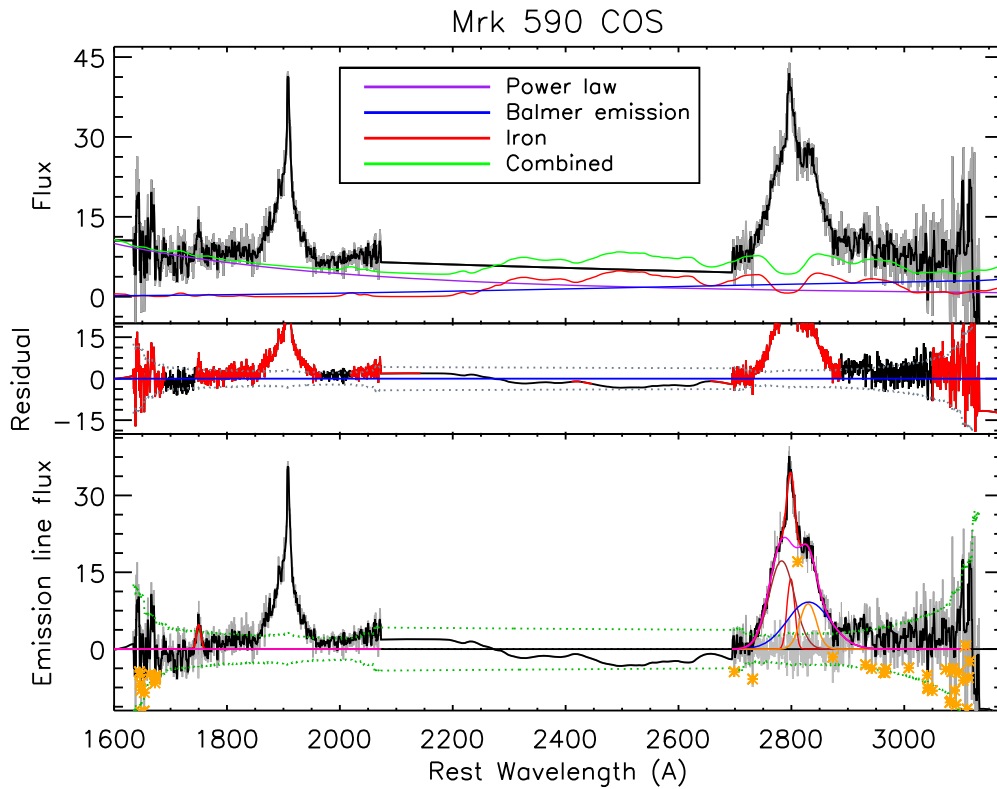


**Figure 5.** *HST*/COS spectrum of Mrk 590 corrected for Milky Way extinction with continuum and line models. Observed flux densities are shown as a function of the rest-frame wavelengths. Top panel: the observed spectrum with the power-law continuum model (purple curve), the Balmer continuum model (blue curve), the iron emission model (red curve), and the sum of the three models (green curve) shown superimposed. Middle panel: residuals obtained by subtracting the continuum, iron, and Balmer emission models shown along with the flux errors (gray dotted curve). Indicated in black are the wavelength regions used to fit the power-law continuum. The Mg II emission line is clearly broad. Bottom panel: emission-line spectrum (black) obtained by subtracting the continuum, iron, and Balmer emission models (shown in the top panel) from the observed spectrum with the line models superimposed. Model fits were made to N III] 1750 Å (red curve) and the broad (magenta curve) and narrow (red curves) components of Mg II. Red curves show the narrow-line components while brown, blue, and yellow curves represent the three Gaussian functions used to model the broad Mg II component (magenta curve). The gray curve (around zero flux level) shows the residuals after subtracting the emission-line model. Yellow stars indicate pixels deviating more than  $3\sigma$  from the rms in the spectrum, which were filtered out prior to the line modeling. The flux errors are shown by the green dotted curve.

here. The main contenders are (1) reflection of the hard X-ray source by the accretion disk (e.g., Crummy et al. 2006); (2) a warm Comptonizing medium around the accretion disk (e.g., Ross et al. 1992; Titarchuk 1994); (3) thermal emission from an accretion disk. Thermal emission from an accretion disk may appear in the soft X-ray band only for relatively low-mass BHs. The re-emergence of the soft excess in the low state, when the hard X-ray emission was weak, suggests that the soft excess is not due to reprocessed hard X-ray emission. An alternative model, in which the soft excess is generated by thermal Comptonization in the optically thick accretion disk corona, is a more likely explanation.

Using a series of observations of Mrk 509, Mehdipour et al. (2011) found that the soft excess is correlated with the UV flux as  $L_{\text{soft excess}} = 1.261(F_{\text{UVW2}})^{2.869}$ , where  $L_{\text{soft excess}}$  is the 0.3–2 keV soft-excess luminosity in units of  $10^{42} \text{ erg s}^{-1}$  and  $F_{\text{UVW2}}$  is the flux in the UVW2 filter in UVOT on *Swift* and OM on *XMM-Newton*, centered at 2030 Å, in units of  $10^{-14} \text{ erg s}^{-1} \text{ cm}^{-2} \text{ Å}^{-1}$ . In our new observations, the soft-excess luminosity of Mrk 590 in the 0.3–2 keV band is  $3.5 \times 10^{40} \text{ erg s}^{-1}$  and the continuum flux at 2030 Å is  $7.7 \times 10^{-16} \text{ erg s}^{-1} \text{ cm}^{-2} \text{ Å}^{-1}$ . The observed soft-excess luminosity is two orders of magnitude larger than that predicted by the Mehdipour relation (correcting the UV flux for the distance of NGC 5548) and shows that the Mehdipour relation between the soft excess and the UV flux is not universal.

The Fe K $\alpha$  emission lines have smaller equivalent widths and smaller fluxes than the values in 2004 reported by Longinotti et al. (2007). This shows that both the neutral and the ionized lines have responded to the continuum changes between 2004 and 2014. This places the reprocessing material within 10 lt-yr or 3 pc of the continuum source, and not from the kiloparsec-scale extended emission region as suggested by Longinotti et al. (2007) for the ionized line.

#### 4.2. The Mg II Emission Line

Our *HST* spectrum clearly shows a broad Mg II emission line. Since we do not have a UV spectrum covering the Mg II line in the low state when the H $\beta$  line had vanished, the presence of the Mg II line in the current spectrum can be interpreted in a couple of different ways.

Photoionization models and evidence from reverberation mapping of the ionization stratification of the broad-line region (BLR) support the co-spatial existence of H $\beta$  and Mg II emitting gas. Thus it is possible that when the broad H $\beta$  emission line disappeared, the broad Mg II line had also disappeared, and now that a broad Mg II line has emerged, possibly a broad H $\beta$  has also emerged. We should note, however, that the response of a line to continuum variations depends not only on the geometry and location of line-emitting region, but also on line responsivity. Cackett et al. (2015) have

shown that the Mg II emission line has very low responsivity compared to other high-ionization emission lines (see also Korista & Goad 2000). It is thus possible that the broad Mg II line had never disappeared. If this is the case, then we cannot comment on the presence of a broad H $\beta$  line in 2014. Roig et al. (2014) found a class of AGNs in the Baryon Oscillation Spectroscopic Survey showing a broad Mg II without a broad H $\beta$ . Wavelength-dependent scattering of the BLR is offered as an explanation by these authors as to why the broad Balmer lines could be missing but the broad Mg II lines are strong. Our results on Mrk 590 suggest that such AGNs may have been in a transition state when H $\beta$  disappeared, but Mg II did not, owing to its low responsivity.

The connection between the soft excess and the emission lines is of interest. In the warm Comptonization model, the seed UV/EUV photons are Compton up-scattered into soft X-rays in the optically thick accretion disk corona. Observationally, the soft excess has been found to correlate with UV emission (e.g., Atlee & Mathur 2009). Thus the emergence of soft excess in Mrk 590 implies a corresponding emergence of the EUV ionizing continuum. This in turn may be responsible for the reappearance of the BLR, which we see with Mg II. This is our preferred model. D14 found the continuum flux at 1450 Å to be  $3.7 \times 10^{-16} \text{ erg s}^{-1} \text{ cm}^{-2} \text{ Å}^{-1}$ , which was two orders of magnitude lower than the IUE value (D14). The 1634 Å flux in our new *HST* data is  $9.2 \times 10^{-16} \text{ erg s}^{-1} \text{ cm}^{-2} \text{ Å}^{-1}$ , which is  $15.1 \times 10^{-16} \text{ erg s}^{-1} \text{ cm}^{-2} \text{ Å}^{-1}$  when extrapolated to 1460 Å. Thus, while the source continues to be in a low state, the UV continuum is re-emerging along with the soft excess. While the presence of the broad Mg II line can be interpreted in different ways, as noted above, it is consistent with the increasing luminosity of the ionizing continuum.

## 5. Conclusion

D14 presented optical, UV, and X-ray observations of the classical Seyfert 1 Mrk 590 that span the past 40+ years. This interesting object brightened by a factor of a few tens between the 1970s and 1990s and then faded by a factor of 100 or more at all continuum wavelengths between the mid-1990s and 2013. Notably, there is no evidence in the current data set that this recent, significant decline in flux is due to obscuration; in particular, the most recent X-ray observations are consistent with zero intrinsic absorption. There were similarly dramatic changes in the emission-line fluxes, the most striking of which is the complete disappearance of the broad component of the H $\beta$  emission line, which had previously been strong (equivalent widths  $\sim 20\text{--}60$  Å).

In this paper we have presented new *Chandra* and *HST* observations from 2014 and we find that Mrk 590 is awakening. While the source continues to be in a low state, its soft excess has re-emerged, though not to the historical level. The broad Mg II emission line is also present. These observations suggest that the soft excess is connected to the UV continuum through warm Comptonization and that the ionizing continuum is also on the rise, but it does not follow the relation between soft excess and UV continuum reported in Mehdipour et al. (2011).

The implications from this long time series of Mrk 590 observations are that (1) Mrk 590 is a direct challenge to the

historical paradigm that AGN type is exclusively a geometrical effect, and (2) there may not be a strict, one-way evolution from Type 1 to Type 1.5–1.9 to Type 2 as recently suggested by Elitzur et al. (2014). Instead, for at least some objects, the presence of BLR emission may coincide with episodic accretion events throughout a single active phase of an AGN. If true, such behavior may be more prominent in Seyfert galaxies, where accretion is likely to be a consequence of secular processes (e.g., Mathur et al. 2012; Martin et al. 2018) and therefore likely more episodic than quasar activity, which may be governed more predominantly by major mergers.

Support for this work was provided by the National Aeronautics and Space Administration through *Chandra* Award Number G04-15114X to S.M. issued by the *Chandra* X-ray Observatory Center, which is operated by the Smithsonian Astrophysical Observatory for and on behalf of the National Aeronautics Space Administration under contract NAS8-03060. Support for the *HST* program number GO-13185 was provided by NASA through a grant from the Space Telescope Science Institute, which is operated by the Association of Universities for Research in Astronomy, Inc., under NASA contract NAS5-26555. K.D.D. was supported by an NSF AAPF fellowship awarded under NSF grant AST-1302093 while she worked on this project. M.V. gratefully acknowledges support from the Danish Council for Independent Research via grant number DFF 4002-00275.

## ORCID iDs

S. Mathur  <https://orcid.org/0000-0002-0129-0316>  
 F. Nicastro  <https://orcid.org/0000-0002-6896-1364>  
 R. W. Pogge  <https://orcid.org/0000-0003-1435-3053>  
 B. M. Peterson  <https://orcid.org/0000-0001-6481-5397>

## References

- Atlee, D., & Mathur, S. 2009, *ApJ*, 703, 1597  
 Cackett, E. M., Gultekin, M., Bentz, M., et al. 2015, *ApJ*, 810, 86  
 Crummy, J., Fabian, A. C., Gallo, L., & Ross, R. R. 2006, *MNRAS*, 365, 1067  
 Denney, K., De Rosa, G., Croxall, K., et al. 2014, *ApJ*, 796, 134  
 Elitzur, M., Ho, L., & Trump, J. 2014, *MNRAS*, 438, 3340  
 Gallo, L., Lehmann, I., Pietsch, W., et al. 2006, *MNRAS*, 365, 688  
 Goad, M. R., Korista, K. T., De Rosa, G., et al. 2016, *ApJ*, 824, 11  
 Gupta, A., Mathur, S., & Krongold, Y. 2015, *ApJ*, 798, 4  
 Korista, K., & Goad, M. . 2000, *ApJ*, 536, 284  
 LaMassa, S., Cales, S., Moran, E., et al. 2015, *ApJ*, 800, 144  
 Longinotti, A., Bianchi, S., Santos-Lieo, M., et al. 2007, *A&A*, 470, 73  
 MacLeod, C., Ross, N., Lawrence, A., et al. 2016, *MNRAS*, 457, 389  
 Martin, G., Kaviraj, S., Volonteri, M., et al. 2018, *MNRAS*, 476, 2801  
 Mathur, S., Fields, D., Peterson, B. M., & Grupe, D. , 2012, *ApJ*, 754, 146  
 Mathur, S., Gupta, A., Page, K., et al. 2017, *ApJ*, 846, 55  
 Mehdipour, M., Branduardi-Raymont, G., Kaastra, J., et al. 2011, *A&A*, 534, 39  
 O'Donnell, J. E. 1994, *ApJ*, 422, 1580  
 Peterson, B. M., Ferrarese, L., Gilbert, K., et al. 2004, *ApJ*, 613, 682  
 Rivers, E., Markowitz, A., Duro, R., & Rothschild, R. , 2012, *ApJ*, 759, 63  
 Roig, B., Blanton, M., & Ross, N. , 2014, *ApJ*, 781, 72  
 Ross, R. R., Fabian, A. C., & Mineshige, S. 1992, *MNRAS*, 258, 189  
 Runnoe, J., Cales, S., Ruan, J., et al. 2016, *MNRAS*, 455, 1691  
 Schlegel, D., Finkbeiner, D., & Davis, M. , 1998, *ApJ*, 500, 525  
 Shappee, B., Prieto, J., Grupe, D., et al. 2014, *ApJ*, 788, 48  
 Titarchuk, L. 1994, *ApJ*, 434, 570  
 Vestergaard, M., & Wilkes, B. 2001, *ApJS*, 134, 1